Theoretical investigation on photoionization from Rydberg states of lithium, sodium and potassium

1976 J. Phys. B: At. Mol. Phys. 9 1279

(http://iopscience.iop.org/0022-3700/9/8/013)

J. Phys. B: Atom. Molec. Phys., Vol. 9, No. 8, 1976. Printed in Great Britain.

Theoretical investigation on photoionization from Rydberg states of lithium, sodium and potassium

M Aymar†, E Luc-Koenig† and F Combet Farnoux‡
†Laboratoire Aimé Cotton, CNRS II, Bâtiment 505, 91405 Orsay, France
‡Equipe de Recherche du CNRS 'Spectroscopie atomique et ionique', Bâtiment 350, 91405 Orsay, France

Received 3 December 1975, in final form 28 January 1976

Abstract. Photoionization cross sections for s, p and d Rydberg states of Li, Na and K have been computed in the framework of a single-electron model (non-relativistic) by using a parametric central potential. The evolution of the non-hydrogenic behaviour of photoionization cross sections near threshold is studied along Rydberg series; non-hydrogenic characters are particularly large for all the *n*s series and for the *n*p series of K. The validity of the method is discussed and it appears that the σ_{np} and σ_{nd} cross sections are more reliable than the σ_{ns} cross sections. Our results are compared to experimental data and other theoretical results, mainly provided by the quantum-defect theory. The agreement between the various results is generally very good for the σ_{np} and σ_{nd} cross sections; the agreement is satisfactory even for the most unfavourable cases provided by the σ_{ns} cross sections of Na and K.

1. Introduction

Photoionization from atomic excited states plays an important role in radiative transfers which appear in laboratory plasmas and hot stellar atmospheres. For the alkali atoms which have low excitation potentials, the population of the excited states is large even at moderate plasma temperatures.

Moreover recent progress in atomic-beam techniques and in tuneable dye laser techniques allows one to obtain high populations in selected excited levels; this is true especially in alkali atoms. From these populated excited levels, photoionization experiments can be performed.

It is, therefore, of particular interest to study photoionization for the excited states of alkali atoms. For these atoms, photoionization cross sections relative to the outermost shell of the ground state are relatively well known from theory and experiment (Marr and Creek 1968, Bardsley 1973), but similar data for excited states are very scarce.

The earlier experimental determinations of cross sections for excited states of alkali atoms were derived from studies of radiative recombination in plasmas; results were obtained in such a way by Mohler (1933) for the 6p ^{2}P states of Cs and by Rothe (1969, 1971) for the 3p ^{2}P states of Na and for the 2p ^{2}P states of Li. More recently, atomic-beam and laser techniques enable one to measure photoionization cross sections directly: Nygaard (1975) has considered the 6p $^2P_{1/2,3/2}$ states of Cs;

experiments on Na are in progress at Laboratoire Aimé Cotton. Photoionization cross sections have already been computed for several excited states (Burgess and Seaton 1960, Moskvin 1963, Ya'akobi 1967, Rudkjøbing 1940, Gezalov and Ivanova 1968, Caves and Dalgarno 1972, Weisheit 1972) but there are no systematic studies of photoionization along a Rydberg series.

In this paper, we present computations concerning photoionization cross sections for s, p and d Rydberg states of light alkali atoms, i.e. Li, Na and K. This study is limited to photoionization near threshold, where non-hydrogenic behaviour is expected (Fano and Cooper 1968). The evolution of this behaviour along a Rydberg series is emphasized. The cross sections are computed, within the framework of a single-electron model (non-relativistic), by use of a central potential. We have employed the parametric potential introduced by Klapisch (1971).

First, the principal formulae are recalled and the fundamental points of the method are examined. Then results are presented and discussed. Finally, comparison is made with other results, mainly those provided by the quantum-defect theory (Burgess and Seaton 1960).

2. Method of calculation

2.1. Photoionization cross sections in a central-field model

Within the framework of a single-particle central-field model (non-relativistic), the cross section (in cm^2) for photoionization from an nl state of a one-electron system is given (see for example Sobel'man 1972 or Stewart 1967) in the dipole approximation by:

$$\sigma_{nl}(\epsilon) = 0{\cdot}855 \times 10^{-18}(\epsilon - \epsilon_{nl})\left(\frac{l}{2l+1}R^2_{nl,l-1}(\epsilon) + \frac{l+1}{2l+1}R^2_{nl,l+1}(\epsilon)\right). \quad (1)$$

Here ϵ_{nl} (<0) is the binding energy of the electron nl and $\epsilon(>0)$ is the energy of the photoelectron; ϵ_{nl} and ϵ are expressed in rydbergs. The energy of the incident photon is $h\nu = \epsilon - \epsilon_{nl}$. For $l \neq 0$, $\sigma_{nl}(\epsilon)$ is the sum of two partial cross sections $\sigma_{nl,l-1}(\epsilon)$ and $\sigma_{nl,l+1}(\epsilon)$ respectively associated with the photoelectron continuum $l-1$ and $l+1$.

The radial matrix elements $R_{nl,l\pm1}(\epsilon)$ are expressed in atomic units. In the dipole length formulation one has:

$$R_{nl,l'}(\epsilon) = \int_0^\infty P_{nl}(r) r P_{\epsilon l'}(r)\,\mathrm{d}r \quad (2)$$

where $P_{nl}(r)$ and $P_{\epsilon l'}(r)$ are the radial wavefunctions of the valence electron in initial and final states. The same central potential $V(r)$ is used to generate $P_{nl}(r)$ and $P_{\epsilon l}(r)$ by solving the Schrödinger equation:

$$\left(\frac{\mathrm{d}^2}{\mathrm{d}r^2} + E - 2V(r) - \frac{l(l+1)}{r^2}\right)P_{El}(r) = 0 \qquad (E = \epsilon_{nl} \text{ or } \epsilon). \quad (3)$$

The numerical factor in equation (1) implies that the continuum wavefunction is normalized per unit energy range, so that:

$$\int_0^\infty P_{\epsilon l}(r) P_{\epsilon' l}(r)\,\mathrm{d}r = \pi\delta(\epsilon - \epsilon'). \quad (4)$$

Then the asymptotic amplitude of $P_{\epsilon l}(r)$ as $r \rightarrow \infty$ is $\epsilon^{-1/4}$.

It is well known that, near the lowest ionization threshold, a hydrogen model of photoionization breaks down because the electrons move in a potential which departs from a pure attractive Coulomb one. Many authors have introduced more realistic potentials (see for example Fano and Cooper 1968, Manson and Cooper 1968, Combet Farnoux 1969 and Bardsley 1973). The simplest potential is the screened Coulomb one used in the quantum-defect theory (Seaton 1958); Burgess and Seaton (1960) have given a general formula for atomic photoionization cross sections in the framework of single-channel theory. In §4.2, comparison is made between results provided by this method and results obtained by the parametric potential method which is now described.

2.2. Parametric potential method applied to calculation of photoionization cross sections

In this work, we use the parametric potential introduced by Klapisch (1971); this potential is particularly well adapted to alkali spectra. It has already been used to compute transition probabilities between discrete states (Aymar 1972). It has also been employed to evaluate photoionization cross sections for the 4d inner shell of Xe (Combet Farnoux 1970).

The parametric potential method, applied to discrete spectra, has been described in detail in many papers (Klapisch 1971, Aymar *et al* 1970) and here, only the fundamental points of this method are recalled. The potential is represented by an analytic function depending on a set of parameters, each parameter describing the distribution of charges in a shell n of the atomic core. The optimal potential is determined by minimizing either the total energy of the lowest state of a given symmetry, or the root-mean-square deviation between observed and calculated energies of selected levels. The results given in this paper are obtained by use of the second criterion; moreover the influence of the chosen potential will be discussed in §3.5.2.

The radial wavefunctions are calculated by numerically solving differential equation (3). We use the Numerov method, with an r-scaled linear mesh similar to the mesh adopted by Herman and Skillman (1963). The mesh is composed of k blocks, each block having N equally spaced intervals; the interval h_0 in the first block is chosen and is doubled in each successive block. The values of k, N and h_0 are judiciously chosen for each nl state; with our program, as many as 5000 values of r can be used. This mesh is more suitable to represent the oscillatory behaviour of continuum radial wavefunctions and of highly excited states than the logarithmic mesh used in the parametric potential method of Klapisch (1971). Moreover Froese Fischer (1971) has shown that the correction term to the Numerov method does not vary with r if the scaled linear mesh is used, while this term increases as r^6 with the logarithmic mesh. Therefore for wavefunctions with an identifiable amplitude at large values of r, the numerical relative error is smaller when the scaled linear mesh is used.

The continuum wavefunctions are normalized (see equation (4)) by using the procedure initially introduced by Strömgren (Rudkjøbing 1940) and described by Stewart (1967). In equation (1), the value of the binding energy ϵ_{nl} is taken to be equal to the opposite of the experimental value of the ionization potential. Cross sections are computed in the energy range from the ionization threshold to 5 Ryd.

3. Results

3.1. Non-hydrogenic behaviour

For hydrogen, $R^{H}_{nl,l'}(\epsilon)$ which can be exactly evaluated (see Bethe and Salpeter 1957), is always a smooth positive monotonically decreasing function of ϵ. Then the photoionization cross section is maximum at threshold and drops to zero as the photon energy increases. For a given Rydberg series, the cross section at threshold increases with n, whereas the cross section at large energy values decreases. The total and partial cross sections at threshold for ns, np and nd Rydberg series of H are plotted against n in figures 1, 2 and 3. The ratio

$$\sigma^{H}_{nl,l-1}(\epsilon)/\sigma^{H}_{nl,l+1}(\epsilon)$$

is always smaller than 1, but increases with n.

For non-hydrogenic atoms, the overlap of $P_{nl}(r)$ and $P_{\epsilon l'}(r)$ is modified with respect to the hydrogen case. Then strong cancellation effects can occur between the positive and the negative contributions to the radial matrix element $R_{nl,l'}(\epsilon)$; $R_{nl,l'}(\epsilon)$ is not necessarily a smooth positive decreasing function of ϵ, becoming negative for some ranges of ϵ. Different curves can be expected for $R_{nl,l'}(\epsilon)$; in figure 4, five typical cases (*a*, *b*, *c*, *d* and *e*) are schematized.

Now, we characterize the $\sigma_{nl,l'}(\epsilon)$ photoionization curve corresponding to each typical profile of $R_{nl,l'}(\epsilon)$:

(*a*) The $\sigma_{nl,l'}(\epsilon)$ curve is hydrogen-like.

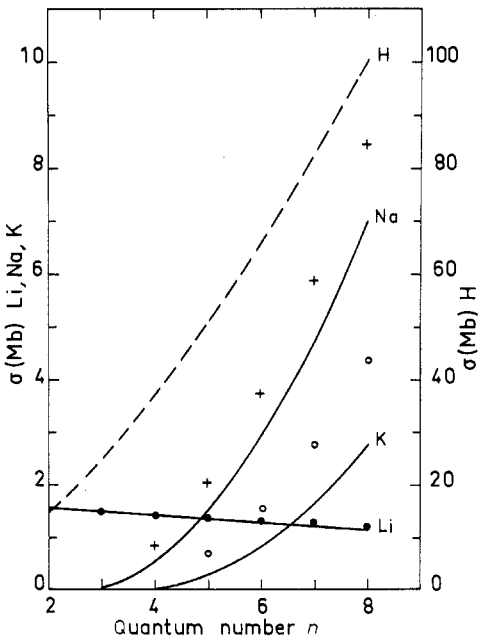

Figure 1. Cross sections at threshold for ns Rydberg series. 1 Mb = 10^{-18} cm^2. Values obtained by the parametric potential method, full curve; values computed in this work by the quantum-defect theory: Li (●), Na (+) and K (○). Different scales are used for $\sigma_{ns}(0)$ of Li, Na and K (left axis) and for $\sigma_{ns}(0)$ of H (right axis).

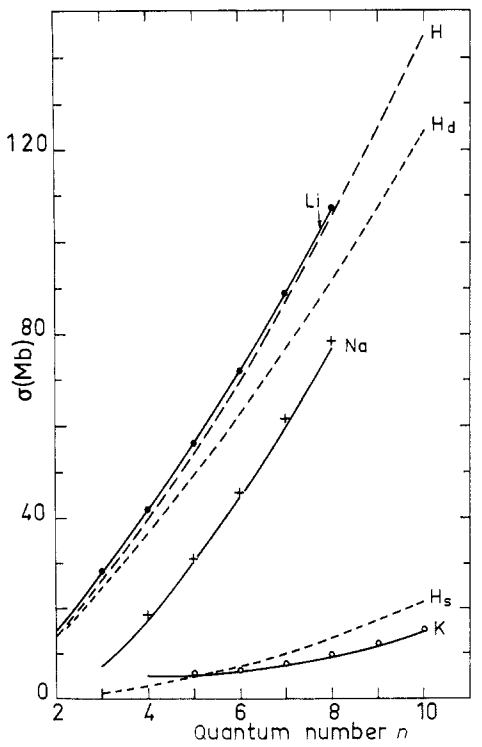

Figure 2. Cross sections at threshold for np Rydberg series. Same notation used as in figure 1. Moreover H_s and H_d correspond respectively to $\sigma^{H}_{np,s}(0)$ and $\sigma^{H}_{np,d}(0)$.

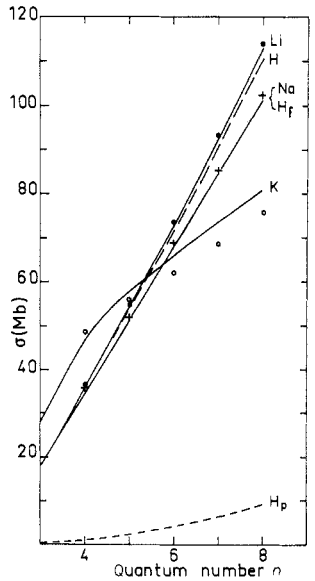

Figure 3. Cross sections at threshold for nd Rydberg series. Same notations as in figure 1. Moreover H_p and H_f correspond respectively to $\sigma^{H}_{nd,p}(0)$ and $\sigma^{H}_{nd,f}(0)$.

(*b*) $\sigma_{nl,l'}(\epsilon)$ shows a maximum near threshold for an energy ϵ_a; this is due to the factor $(\epsilon - \epsilon_{nl})$ which appears in equation (1) (figure 4(*b*)).

(*c*) $\sigma_{nl,l'}(\epsilon)$ decreases from threshold to a minimum at energy ϵ_1 and then reaches a flat maximum at higher energy ϵ_a (figure 4(*c*)).

(*d*) $\sigma_{nl,l'}(\epsilon)$ shows a maximum near threshold for an energy ϵ_b (due to the maximum negative value of $R_{nl,l'}(\epsilon)$), then shows a zero minimum at energy ϵ_1 and a second flat maximum at energy ϵ_a (figure 4(*d*)).

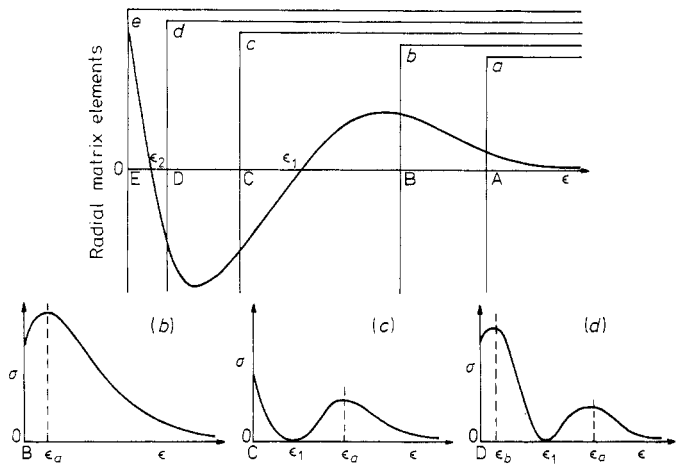

Figure 4. Radial matrix elements and cross sections against energy for some typical cases. In the upper figure 4(*a*), five typical cases (*a*, *b*, *c*, *d* or *e*) of $R_{nl,l'}(\epsilon)$ are schematized. These cases correspond to a threshold energy ($\epsilon = 0$) located respectively at A, B, C, D or E. In each case, only the part of the curve at the right of the corresponding vertical axis is meaningful; the left part must not be used to study oscillator strengths. The lower figures 4(*b*), 4(*c*) and 4(*d*) show the $\sigma_{nl,l'}(\epsilon)$ curves corresponding respectively to cases *b*, *c* and *d* of the upper figure.

(*e*) This case, corresponding to a radial matrix element with two zeros, will be discussed later in §3.3.3.

The cases (*a*)–(*d*) were largely described by Fano and Cooper (1968). The minimum at energy ϵ_1 is generally called a 'Cooper minimum'. Experimental photoionization curves corresponding to these cases were encountered for many atoms, in particular for alkali atoms, in a large energy range from the visible to soft x-ray regions. The case (*e*) was recently pointed out by Msezane and Manson (1975) in theoretical investigations on photoionization of Cs 5d.

In fact, these five profiles occur in this study. For $l \neq 0$, the combination of two curves, one corresponding to $\sigma_{nl,l-1}(\epsilon)$ and the other one corresponding to $\sigma_{nl,l+1}(\epsilon)$, gives different shapes to the $\sigma_{nl}(\epsilon)$ curve. The behaviour (hydrogenic or not) will now be described in greater detail for each *nl* Rydberg series.

3.2. *ns series* ($n \leqslant 8$)

The non-hydrogenic character of σ_{ns} cross sections from the ground state of alkali atoms is well known (Fano and Cooper 1968). Let us recall that the photoionization curve is of type (*b*) for Li 2s and of type (*c*) for Na 3s and K 4s (Hudson and Carter 1965, 1967, Marr and Creek 1968).

For the excited *n*s states of these atoms, the non-hydrogenic characteristics of $\sigma_{ns}(\epsilon)$ are qualitatively the same. For Li, the cross sections at threshold decrease slightly with *n*, as can be seen from figure 1. With increasing values of *n*, the maximum is shifted towards threshold, but does not disappear even for large values of *n*; moreover $\sigma_{ns}(\epsilon_a)/\sigma_{ns}(0)$ remains nearly constant with *n* (for notation see figure 4(*b*)).

For Na and K the cross section at threshold increases with *n* (see figure 1) whereas $\sigma_{ns}(\epsilon_a)$ decreases very quickly with *n*; for example, in the case of Na, $\sigma_{ns}(\epsilon_a)/\sigma_{ns}(0)$ is larger than 1 for $n = 3$ and is approximately 10^{-3} for $n = 8$. Although σ_{ns} has a very low maximum for higher excited *n*s states, the non-hydrogenic character does not disappear because the values of the energy ϵ_1 and ϵ_a are almost stationary for large values of *n* (for notation see figure 4(*c*)).

For a given *n* value, cross sections near threshold are always 10 to 100 times smaller than the hydrogen ones (notice in figure 1 the modified scale used for hydrogen cross sections). In fact, large cancellation effects occur in the radial matrix elements. This point will be discussed in §3.5.2.

3.3. *np series*

In all cases, $\sigma_{np,s}(\epsilon)$ has a hydrogen-like profile (type (*a*)), but the variation of $\sigma_{np,d}(\epsilon)$ is different for each alkali atom.

3.3.1. Li ($n \leqslant 8$). For Li, $\sigma_{np,d}(\epsilon)$ is practically equal to $\sigma^{H}_{np,d}(\epsilon)$; $\sigma_{np,s}(\epsilon)$ is larger than $\sigma^{H}_{np,s}(\epsilon)$ but is much smaller than $\sigma_{np,d}(\epsilon)$. Consequently, for given values of *n* and ϵ, the $\sigma_{np}(\epsilon)$ cross section of Li is close to the $\sigma^{H}_{np}(\epsilon)$ cross section of H. The cross sections at threshold are reported in figure 2.

3.3.2. Na ($n \leqslant 8$). The partial and total cross sections for photoionization from the 3p state of Na are shown in figure 5(*a*). The curve for partial $\sigma_{np,d}(\epsilon)$ cross section is of type (*c*) (see figure 4(*c*)); the maximum at energy ϵ_a is very low since $\sigma_{np,d}(0)/\sigma_{np,d}(\epsilon_a) = 150$. However, since the contribution of $\sigma_{np,s}(\epsilon)$ is not negligible, the total cross section

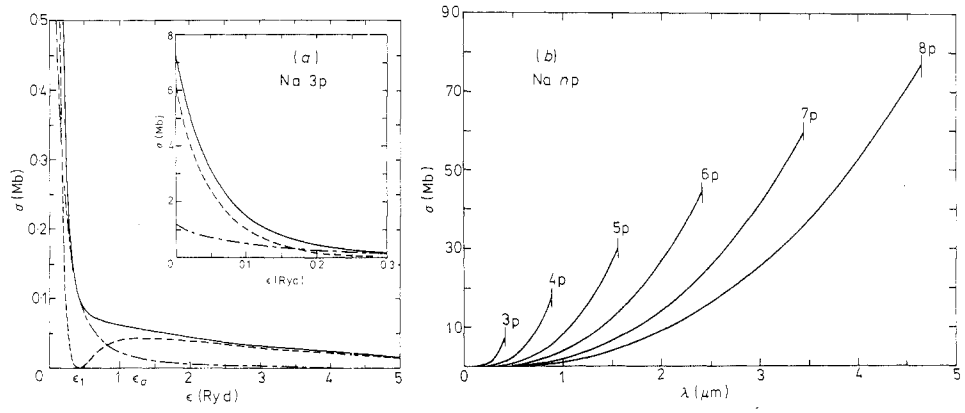

Figure 5. (*a*) Partial and total cross section curves for Na 3p. $\sigma_{3p,s}(\epsilon)$: chain curve; $\sigma_{3p,d}(\epsilon)$: broken curve; $\sigma_{3p}(\epsilon)$: full curve. (*b*) Cross sections against wavelength for the *n*p series of Na.

exhibits no minimum at all but only a slope discontinuity near the energy ϵ_1 corresponding to the zero minimum of $\sigma_{np,d}(\epsilon)$. In the energy range near threshold, where the cross section is large, the behaviour is hydrogen-like; however the decrease with energy is quicker than in the hydrogen case.

For $n > 3$, the curves of $\sigma_{np}(\epsilon)$ cross sections show the same characteristics as for $n = 3$. However $\sigma_{np}(0)$ increases with n, while $\sigma_{np}(\epsilon_a)$ decreases very quickly. In figure 2 it can be seen that the cross section at threshold is slightly smaller than the hydrogen one, for a given value of n. In figure 5(*b*), photoionization cross sections for the *n*p series of Na have been plotted against wavelength.

3.3.3. K ($n \leqslant 10$). The partial $\sigma_{np,d}(\epsilon)$ cross section is of type (*d*) or (*e*) with two maxima at energies ϵ_a and ϵ_b (see figure 4(*d*)). As n increases, $\sigma_{np,d}(\epsilon_b)$ decreases quickly while $\sigma_{np,s}(0)$ increases; therefore, near threshold, the relative weight of the two partial cross sections varies strongly with n. For large values of n, the total cross section is mainly related to the partial $\sigma_{np,s}(\epsilon)$ cross section and the $\sigma_{np}(\epsilon)$ of K is of the same order of magnitude as the corresponding partial $\sigma^{H}_{np,s}(\epsilon)$ cross section of H (see figure 2).

Figure 6 shows the partial and total cross sections for the two extreme cases studied here ($n = 4$ and $n = 10$) in the energy range near threshold. The progressive

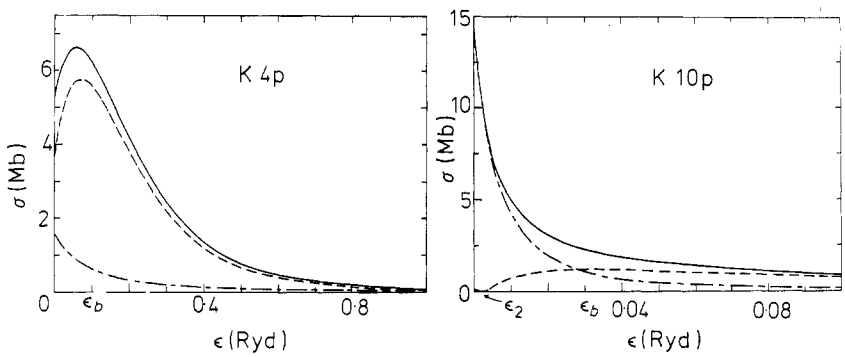

Figure 6. Partial and total cross section curves for K 4p and K 10p. $\sigma_{np,s}(\epsilon)$: chain curve; $\sigma_{np,d}(\epsilon)$: broken curve; $\sigma_{np}(\epsilon)$: full curve.

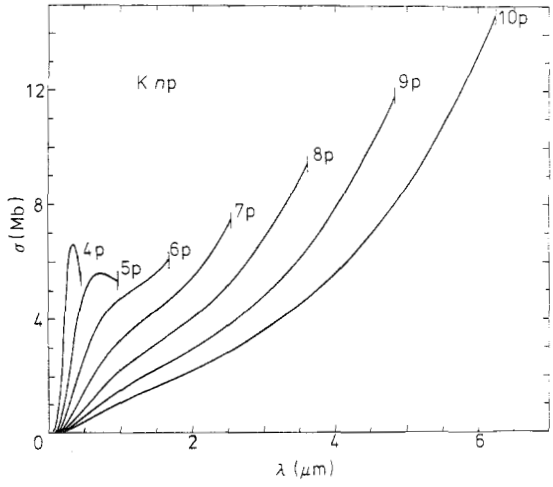

Figure 7. Cross sections against wavelength for the np series of K.

change of shape for photoionization curves, for increasing values of n, can be seen in figure 7, where cross sections have been plotted against wavelength for the np series of K.

Let us now give some comments on the dipole matrix elements $R_{np,d}(\epsilon)$. For $n \leqslant 9$ the $R_{np,d}(\epsilon)$ curve is of type (*d*), while $R_{10p,d}(\epsilon)$ is of type (*e*) with two zeros (see figure 4). Our calculated results for $R_{10p,d}(\epsilon)$ are shown in figures 8(*a*) and (*b*). The Cooper minimum (for $\epsilon = \epsilon_1$) and the second very low maximum (for $\epsilon \simeq \epsilon_a$) occur in the energy range where the total cross section is very small (notice the differences of scale between figures 8(*a*) and (*b*)).

The $R_{10p,d}(\epsilon)$ curve for K shows the same features as the $R_{5d,f}(\epsilon)$ for Cs, which was recently computed by Msezane and Manson (1975). However, the total cross section curves $\sigma_{10p}(\epsilon)$ of K and $\sigma_{5d}(\epsilon)$ of Cs are different: in the case of Cs 5d,

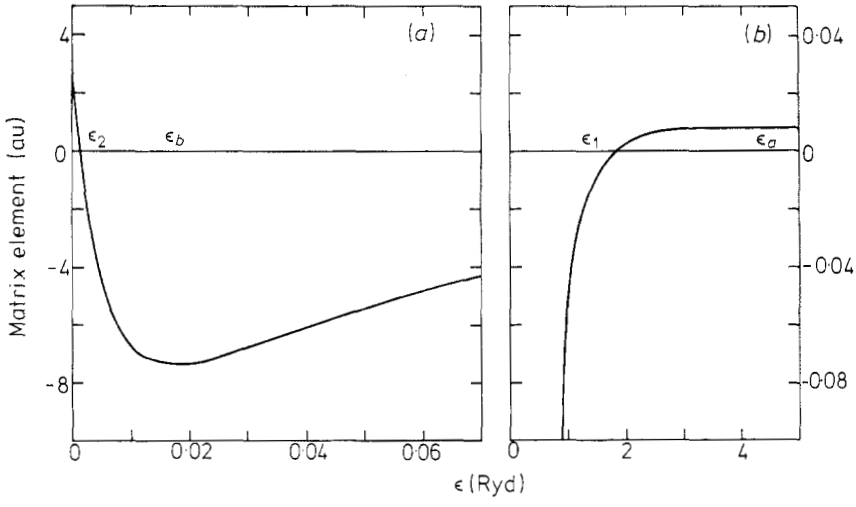

Figure 8. Radial matrix element $R_{10p,d}(\epsilon)$ for K 10p. (*a*) Energy range: $0 < \epsilon < 0{\cdot}07$ Ryd; (*b*) energy range: $0{\cdot}9 < \epsilon < 5$ Ryd. Note the different scales used in the two figures. In the intermediate energy range ($0{\cdot}07 < \epsilon < 0{\cdot}9$ Ryd) $R_{10p,d}(\epsilon)$ is a negative monotonically increasing function of ϵ.

two minima of $\sigma_{5d}(\epsilon)$ are predicted for the energies where $\sigma_{5d,f}(\epsilon)$ vanishes; in the case of K 10p, such minima do not appear because the zeros of $\sigma_{10p,d}(\epsilon)$ occur at energies where the other partial cross section $\sigma_{10p,s}(\epsilon)$ is large.

3.4. *nd series* ($n \leqslant 8$)

In all cases, $\sigma_{nd,f}(\epsilon)$ is much larger than $\sigma_{nd,p}(\epsilon)$ and the profile of the $\sigma_{nd}(\epsilon)$ curve is always determined by the $\sigma_{nd,f}(\epsilon)$ profile which is hydrogen-like (type (*a*)).

For Li, the two partial cross sections are nearly equal to the corresponding hydrogen ones, for given values of n and ϵ. For Na, $\sigma_{nd,f}(\epsilon)$ is still equal to $\sigma^{H}_{nd,f}(\epsilon)$. Moreover, $\sigma_{nd,p}(\epsilon)$ is quite negligible because strong cancellation effects occur in the corresponding radial matrix element. Then the total $\sigma_{nd}(\epsilon)$ cross section of Na is very close to the partial $\sigma^{H}_{nd,f}(\epsilon)$ cross section of H.

For K, both $\sigma_{nd,p}(\epsilon)$ and $\sigma_{nd,f}(\epsilon)$ cross sections differ from the corresponding hydrogen ones but the $\sigma_{nd}(\epsilon)$ cross sections are of the same order of magnitude as the $\sigma^{H}_{nd}(\epsilon)$ cross sections of H. However the decrease of cross section with energy is slower than in the hydrogen case.

The cross sections at threshold for the three nd series are plotted against n in figure 3. It is interesting to remark that, for Na and K, we find again a non-hydrogenic character already pointed out by Msezane and Manson (1975): the $\sigma_{nd,p}(\epsilon)$ curve of photoionization corresponding to $l \rightarrow l-1$ transition shows a Cooper minimum. However, this point is only of theoretical interest because the minimum is always hidden by the $\sigma_{nd,f}(\epsilon)$ photoionization cross section which is much larger.

The $\sigma_{nd}(\epsilon)$ curves are not shown in this paper, since they do not differ much from the hydrogen ones; however these results are available at Laboratoire Aimé Cotton.

3.5. *Discussion*

3.5.1. Length and velocity formulations. In §2.1, cross sections are expressed in terms of the dipole length operator; the dipole velocity operator can also be used. In the one-electron approximation, if the same potential is used for generating the initial state and the final one, and if the experimental ϵ_{nl} value (ϵ^{exp}_{nl}) is used, two different cross section values $\sigma^{r}_{nl}(\epsilon)$ (length) and $\sigma^{\nabla}_{nl}(\epsilon)$ (velocity) can be obtained. They are connected by the following expression:

$$\sigma^{\nabla}_{nl}(\epsilon) = \left(\frac{\epsilon - \epsilon^{th}_{nl}}{\epsilon - \epsilon^{exp}_{nl}}\right)^2 \sigma^{r}_{nl}(\epsilon)$$

where ϵ^{th}_{nl} is the eigenvalue associated with $P_{nl}(r)$. In all the cases studied here, the relative difference between $\sigma^{r}_{nl}(\epsilon)$ and $\sigma^{\nabla}_{nl}(\epsilon)$ is small ($<15\%$) and decreases with ϵ and n.

3.5.2. Potential. In the parametric potential method, for a given spectrum, different central potentials could be optimized according to the chosen criterion. The comparison of cross sections computed with different potentials provides a test of validity for our results.

The σ_{np} and σ_{nd} cross sections are of the same order of magnitude as the corresponding hydrogen ones. Therefore, these cross sections are not very sensitive to

a small change of wavefunctions, i.e. to the choice of the potential. In this study the various cross sections corresponding to different potentials are in good agreement; in the worst case the relative difference does not exceed 10%.

The σ_{ns} cross sections are ten to a hundred times smaller than the corresponding hydrogen ones. Then these cross sections are very sensitive to a small change of wavefunctions as often noticed, in particular, by Burgess and Seaton (1960); indeed strong cancellation effects occur between positive and negative contributions to the radial matrix elements $R_{ns,p}(\epsilon)$.

In order to improve the σ_{ns} cross sections, one has to use a more elaborate model. In alkali atoms it is well known that photoabsorption is strongly affected by core polarization effects (Hameed *et al* 1968). When the ground state of the core has spherical symmetry, it is possible to obtain more realistic wavefunctions for the valence electron by adding effective terms to the central potential; these terms describe the long-range polarization interaction between core and valence electrons (see the references given in Bardsley 1973). Core polarization effects have also been included by means of the 'polarized orbital method' (LaBahn and Garbaty 1974) or by use of many-body perturbation theory (Chang and Kelly 1975, Chang 1974). The introduction of such effects in our model is in progress.

4. Comparison with other results

4.1. Ground states

Except for the experimental investigations on photoionization from Li 2p (Rothe 1971) and Na 3p (Rothe 1969), experimental data are only available for photoionization from the ground state. Unfortunately, as already noticed, it is rather difficult to obtain accurate theoretical values of the photoionization cross sections for *n*s states; therefore, comparison between experimental and theoretical data for photoionization from the ground state does not allow one to test the validity of the other results.

For Li 2s, our results are in rather good agreement with experimental data (Hudson and Carter 1967). Near the ionization threshold of Na 3s and K 4s, our results, although depending on the choice of the potential, are consistent with both experimental and theoretical data (Hudson and Carter 1965, 1967, Marr and Creek 1968, Bardsley 1973). On the short wavelength side of the minimum our values seem to agree well with other calculations based on the use of a single-particle model, but all these results are smaller than the experimental ones. All important correlation effects have been studied in great detail by the use of many-body perturbation theory (Chang 1974, Chang and Kelly 1975). The improvement of the results is rather small considering the great complexity of this method; furthermore, these calculations are not able to reproduce exactly the experimental data over the whole energy range.

4.2. Excited states

For existed states the only available experimental data are those derived from the radiative recombination studies by Rothe; these results concern photoionization near threshold for Na 3p (Rothe 1969) and for Li 2p (Rothe 1971). However theoretical cross sections for several excited states have been computed by various methods. Burgess and Seaton (1960), Moskvin (1963) and Ya'akobi (1967) used the quantum

Table 1. Experimental and calculated cross sections (Mb) at threshold; comparison with previous results.

		Present work	Previous theoretical results						Experimental results
		1	2	3	4	5	6	7	8
Li	3s	1·48		1·27	1·42		1·17	1·42	
	4s	1·40					1·31		
	5s	1·33					0·811		
	2p	15·20		15·70	16·40		15·00	15·40	19·7 ± 3†
	3p	28·10			10·00		28·20	28·00	
	4p	41·70					34·20		
	5p	56·20					43·20		
	3d	18·20			150·00		17·50		
	4d	36·20					30·60		
Na	4s	0·54	0·90	0·90		0·16			
	3p	7·38	8·10	6·30		7·70			7·63 ± 0·9‡
	4p	17·50	18·80			16·10			
K	5s	0·27		0·52					
	4p	5·35		4·80					
	3d	28·30		35·00					

1 Present work—parametric potential method; 2 Burgess and Seaton (1960); 3 Moskvin (1963); 4 Ya'akobi (1967); 5 Rudkjøbing (1940); 6 Gezalov and Ivanova (1968); 7 Caves and Dalgarno (1972); 8 †Rothe (1971); ‡Rothe (1969).

defect theory. Rudkjøbing (1940) and Gezalov and Ivanova (1968) carried out calculations using a self-consistent approximation including exchange terms. Caves and Dalgarno (1972) employed a semi-empirical potential including core polarization effects.

The experimental and calculated cross sections at threshold are reported in table 1. The previous theoretical results are either those quoted by the authors or those obtained from their published curves.

The cross section values determined in this work are in general agreement with those obtained in both theoretical and experimental work. However the discrepancy is largest for the *n*s states; remember that this is the most unfavourable case. For Li 3p and Li 3d the large discrepancy between the results of Ya'akobi (1967) and the other ones cannot be explained. For highly excited states of Li the values obtained by Gezalov and Ivanova (1968) are smaller than the present ones; nevertheless for energies larger than 0·02 Ryd, the agreement is very good. In fact for the continuum wavefunctions, the normalization procedure used by these authors cannot be employed at threshold, because of the different asymptotic limit of the corresponding wavefunction; the extrapolation formula used by Gezalov and Ivanova (1968) seems to be inadequate for large n values because of the fast decrease from threshold.

In the two cases where experimental data are available (Rothe 1969, 1971) the various theoretical results are in good agreement among themselves. For Na 3p theoretical results agree well with the experimental data. For Li 2p, the computed cross sections are a little bit smaller than the experimental ones; the discrepancy is not too large when taking into account the experimental uncertainty.

For highly excited states, no previous theoretical results are available; however the general formula given by Burgess and Seaton (1960) can be used for computing these cross sections. This formula is employed here to calculate $\sigma_{nl}(0)$ for all states

such as $\nu_{nl} \geqslant l + 2$ (ν_{nl} is the principal quantum number given by $\epsilon_{nl} = -1/\nu_{nl}^2$). The corresponding values of $\sigma_{nl}(0)$, shown in figures 1–3, are in good agreement with those determined by using the central parametric potential; the discrepancy is not too large even for the worst cases provided by the σ_{ns} cross sections of Na and K.

5. Conclusion

In this work, we have studied the non-hydrogenic behaviour of photoionization from Rydberg states of the lightest alkali atoms. The non-hydrogenic features are particularly significant for all the ns series and for the np series of K even for large values of n.

The cross sections of photoionization from np and nd states are close to the corresponding cross sections of atomic hydrogen or else they are of the same order of magnitude. These values are not sensitive to small changes of wavefunctions and when comparison with other results is possible, the agreement is generally rather good. Therefore we are allowed to expect that all computed σ_{np} and σ_{nd} values are good approximations of the true cross sections.

The cross sections for photoionization from ns states are less reliable, because strong cancellation effects occur in the radial matrix elements. However, the gross spectral shape of cross sections and the systematic trend along a Rydberg series are probably correctly predicted.

Results provided by the central-field method are often similar to those obtained by the quantum-defect theory of Burgess and Seaton (1960) essentially for the np and nd series of the light alkali atoms. However, our method permits several extensions which could not be introduced in the framework of single-channel quantum-defect theory. Some extensions of this work are now in progress: introduction of core polarization effects (in particular to improve the σ_{ns} cross sections), and relativistic generalization (in particular to interpret the non-zero minimum of $\sigma_{4s}(\epsilon)$ of K and to investigate photoionization in heavy alkali atoms, expecially in Cs).

References

Aymar M 1972 *Physica* **57** 178–90
Aymar M, Crance M and Klapisch M 1970 *J. Physique Coll.* **31** C4 141–8
Bardsley J N 1973 *Case Studies in Atomic Physics* vol 4, ed E W McDaniel and M R C McDowell (Amsterdam: North-Holland) pp 299–368
Bethe H A and Salpeter E E 1957 *Quantum Mechanics of One and Two Electron Atoms* (Berlin: Springer Verlag)
Burgess A and Seaton M J 1960 *Mon. Not. R. Astron. Soc.* **120** 121–51
Caves T C and Dalgarno A 1972 *J. Quant. Spectrosc. Radiat. Transfer* **12** 1539–52
Chang J J and Kelly H P 1975 *Phys. Rev.* A **12** 92–8
Chang T N 1974 *J. Phys. B: Atom. Molec. Phys.* **8** 743–50
Combet Farnoux F 1969 *J. Physique* **30** 521–30
——1970 *J. Physique Coll.* **31** C4 203–9
Fano U and Cooper J W 1968 *Rev. Mod. Phys.* **40** 441–507
Froese Fischer C 1971 *Comp. Phys. Commun.* **2** 124–6
Gezalov Kh B and Ivanova A V 1968 *High Temp.–High Press.* **6** 400–4
Hameed S, Herzenberg A and James M G 1968 *J. Phys. B: Atom. Molec. Phys.* **1** 822–30

Herman F and Skillman S 1963 *Atomic Structure Calculations* (Englewood Cliffs, New Jersey: Prentice Hall)
Hudson R D and Carter V L 1965 *Phys. Rev.* **139** 1426–8
——1967 *J. Opt. Soc. Am.* **57** 651–4
Klapisch M 1971 *Comp. Phys. Commun.* **2** 239–60
LaBahn R W and Garbaty E A 1974 *Phys. Rev.* A **9** 2255–8
Manson S T and Cooper J W 1968 *Phys. Rev.* **165** 126–38
Marr G V and Creek D M 1968 *Proc. R. Soc.* A **304** 233–44
Mohler F L 1933 *J. Res. NBS* **10** 771–80
Moskvin Yu V 1963 *Opt. Spectrosc.* **15** 316–7
Msezane A and Manson S T 1975 *Phys. Rev. Lett.* **35** 364–6
Nygaard K J 1975 *Phys. Rev.* A **12** 1440–7
Rothe D E 1969 *J. Quant. Spectrosc. Radiat. Transfer* **9** 49–62
——1971 *J. Quant. Spectrosc. Radiat. Transfer* **11** 355–65
Rudkjøbing M 1940 *Publ. Kbh. Obs* **18** 1–15
Seaton M J 1958 *Mon. Not. R. Astron. Soc.* **118** 504–18
Sobel'man I I 1972 *An Introduction to the Theory of Atomic Spectra* (Oxford: Pergamon Press)
Stewart A L 1967 *Adv. Atom. Molec. Phys.* **3** 1–51
Weisheit J C 1972 *J. Quant. Spectrosc. Radiat. Transfer* **12** 1241–8
Ya'akobi 1967 *Proc. Phys. Soc.* **92** 100–6